



# Preliminary study of total variation noise reduction algorithm with high-energy industrial X-ray imaging system in nondestructive testing field

Heemoon Cho<sup>a</sup>, Youngjin Lee<sup>b,\*</sup>

<sup>a</sup> FutureChem Co. Ltd., 21, Gwanjeodong-ro, Yeonmujang 3-gil, Seongdong-gu, Seoul, Republic of Korea

<sup>b</sup> Department of Radiological Science, College of Health Science, Gachon University, 191, Hambakmoero, Yeonsu-gu, Incheon, Republic of Korea

## ARTICLE INFO

### Keywords:

Nondestructive testing (NDT)  
High-energy industrial X-ray system  
Total variation (TV) approach  
Noise reduction algorithm  
Quantitative evaluation of image performance

## ABSTRACT

Over the past years, many studies have evaluated the performance of nondestructive testing high-energy X-ray imaging methods. In these high-energy industrial X-ray imaging systems, the noise is very important when accurately assessing the nondestructive analysis of faults inside the object volume. A common way to improve the noise performance is the total variation (TV) noise reduction algorithm. Thus, the purpose of this study is to establish a high-energy industrial X-ray imaging system using 450 kVp energy and to confirm the feasibility of our designed TV noise reduction algorithm. We used an X-ray generator (including source, power supply, and cooler) and a flat panel detector made of an amorphous silicon material. In addition, we acquired the X-ray image for a battery and an air pump and then applied our designed TV noise reduction algorithm to these images. To evaluate the image performance, we used normalized noise power spectrum (NNPS), contrast to noise ratio (CNR), and coefficient of variation (COV). According to the NNPS result, the noise performance of our method was improved compared to conventional noise reduction methods. In addition, the CNR of our TV noise reduction algorithm was 1.58, 1.30, and 1.26 times greater than that achieved for the noisy image, median filter and Wiener filter, respectively. We also acquired excellent COV results for the high-energy X-ray imaging system (about 1.93 times higher than that of the noisy image). Our results suggest that a TV noise reduction algorithm can be constructed with an improved image performance in high-energy industrial X-ray imaging systems.

## Introduction

Since X-rays were discovered in 1895 by W. Roentgen, X-ray-based imaging systems have been used widely in medical treatment and industry [1–3]. Especially, industrial X-rays are a form of nondestructive testing (NDT) and can be employed to confirm the existence of faults in the internal structure of specimens and the material composition in the scanned volume part [3–5]. In industrial X-ray imaging systems, the most commonly used high-energy X-ray beams have energies of 450 kVp or 3 MeV (up to 15 MeV) using < 0.5 mm resolving power [6,7].

The image quality is the faithfulness of the representation of the imaged object and is very important for the improvement of the accuracy for internal structure information in industrial X-ray imaging systems [3]. All industrial X-ray images, including high-energy beams, contain some visual noise that is significant in this system. Although noise can degrade the image quality, the most significant factor is that noise can be reduced in various ways using both hardware (development of newly-designed detector materials or acquiring a high radiation dose) and software [8,9]. With the rapid advance of computer science

and engineering, software methods with image processing denoising techniques have been actively used to improve the noise performance. Recently, many studies have been conducted for the feasibility of the total variation (TV) noise reduction algorithm based on an iterative method in the field of medical imaging [10–12]. This algorithm is an effective noise reduction method for recovering signals and was introduced by Rudin, Osher, and Fatemi in 1992 [10]. In addition, this algorithm is defined by the minimization of a nondifferentiable function and is based on a nonlinear filtering method. Although many studies of the feasibility of TV noise reduction algorithm in medical imaging have been performed, few studies have been conducted to confirm the application in industrial X-ray imaging. In this study, we establish a high-energy industrial X-ray imaging system and evaluate the image performance of the TV noise reduction algorithm in an industrial X-ray image. For that purpose, we used normalized noise power spectrum (NNPS), contrast to noise ratio (CNR), and coefficient of variation (COV) to evaluate quantitatively the image performance in our established system with the TV noise reduction algorithm.

\* Corresponding author.

E-mail address: [yj20@gachon.ac.kr](mailto:yj20@gachon.ac.kr) (Y. Lee).

<https://doi.org/10.1016/j.rinp.2018.06.036>

Received 28 May 2018; Received in revised form 12 June 2018; Accepted 15 June 2018

Available online 21 June 2018

2211-3797/ © 2018 The Authors. Published by Elsevier B.V. This is an open access article under the CC BY license

(<http://creativecommons.org/licenses/by/4.0/>).

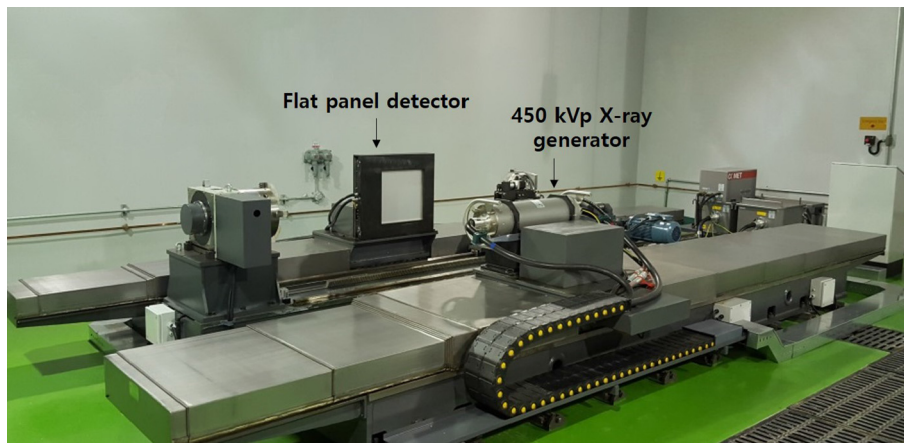


Fig. 1. Photo of our 450 kVp industrial X-ray system. This system consists of a flat panel detector and X-ray generator. Our system has a slide base carrying the X-ray source and the detector.

**Materials and methods**

*Established high-energy industrial X-ray imaging system*

In this study, we focus on the development of high-energy industrial X-ray imaging system using a 450 kVp beam. Fig. 1 shows the overall established 450 kVp industrial X-ray imaging system. This system consists of an X-ray generator, a flat panel detector, and a chuck for mounting a large object.

We used a bipolar metal-ceramic X-ray tube for the 450 kVp X-ray generator with a high voltage power supply and a cooler. Fig. 2 and Table 1 show the schematic diagram and specifications, respectively, of the X-ray generator. In addition, we used an amorphous silicon flat panel detector with a 200 μm pixel size using 2048 × 2048 pixels (total active area: 409.6 mm × 409.6 mm).

*Total variation (TV) noise reduction algorithm modelling*

In X-ray-based imaging systems, the main task of the noise reduction algorithm is to create a clear image from a noisy image. To address this problem, a variety of techniques have been developed using principles that minimizes the gradient of an X-ray image. Among these

**Table 1**

Specifications of the used 450 kVp X-ray generator.

Parameter	Value
Focal spot size (mm)	0.4/1.0
Voltage (kV)	20–450
Current (mA)	0.01–15
Cooling material	Oil

principles, the TV regularization technique is widely used in the field of X-ray imaging and was first researched by Rudin, Osher, and Fatemi for Gaussian noise reduction. Especially, the TV noise reduction algorithm based on the regularization technique with the L<sub>1</sub>-norm estimation was used in this study because of the easier computation and analysis processing. Given a noisy image and a restored image, the TV model considers the solution for the convex optimization problem.

The basic equation of image degradation process with noise characteristics is calculated as follows:

$$A(x, y) = h(x, y) ** PSF(x, y) + N(x, y) (**: 2D convolution) \tag{1}$$

where  $A(x, y)$  is the image after degradation,  $h(x, y)$  is the original image,  $PSF(x, y)$  is the shift-invariant point spread function, and

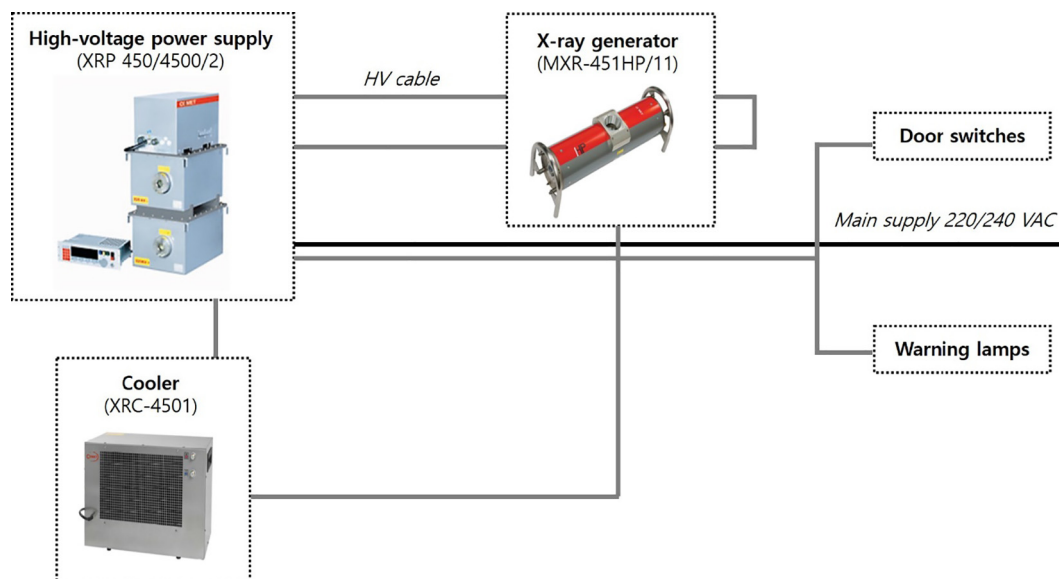


Fig. 2. Schematic diagram of the X-ray generator, which consists of a high-voltage power supply (XRP 450/4500/2), source generator (MXR-451HP/11), and cooler (XRC-4501).

$N(x, y)$  is the noise. A general method for solving unknown term  $h(x, y)$  is regularization function and basic equation of our proposed noise reduction algorithm using smoothing function,  $u_s$ , based on TV is calculated as follows [10]:

$$V_{TV}[u_s] = \int_{\Omega} |\nabla u_s| dx dy (\nabla u_s = \sqrt{u_{sx}^2 + u_{sy}^2}) \quad (2)$$

where  $V_{TV}$  is the total variation,  $\nabla u_s$  is the gradient, and  $u_{sx}$  and  $u_{sy}$  are the  $\partial u_s / \partial x$  and  $\partial u_s / \partial y$ , respectively. To cope with “ $V_{TV}[u_s] \rightarrow \min$ ” problem, new equation can be expressed as shown below:

$$\int_{\Omega} (v - u_s)^2 dx dy = \text{constant} \quad (3)$$

Based on  $V_{TV}$  equation, denoising models for rejecting distribution of Gaussian ( $u_G$ ) and Poisson ( $u_P$ ) noises are calculated as follows:

$$u_G = \text{argmin} \left[ \int_{\Omega} |\nabla u_s| dx dy + \frac{\lambda}{2} \int_{\Omega} (v - u_{sm})^2 dx dy \right] \quad (\text{Lagrange multiplier: } \lambda > 0) \quad (4)$$

$$u_P = \text{argmin} \left[ \int_{\Omega} |\nabla u_s| dx dy + \beta \int_{\Omega} u_s - v \ln(u_s) dx dy \right] \quad (\text{regularization coefficient: } \beta > 0) \quad (5)$$

To compare the image performance between TV and previously developed noise reduction algorithms, we also designed conventional algorithms using both a median, and Wiener filter with a nonlinear and statistical method, respectively.

*Quantitative evaluation of image performance*

The capabilities of the designed TV noise reduction algorithm were evaluated by applying it to a developed high-energy industrial X-ray imaging system using a 450 kVp beam and calculating the NNPS, CNR, and COV. NPS is used to evaluate noise characteristics in X-ray images and is defined as the variance per frequency in the spatial frequency domain. NPS is calculated as follows [13]:

$$\begin{aligned} \text{NPS}(u_n, v_k) &= \lim_{N_x, N_y \rightarrow \infty} (N_x N_y \Delta x \Delta y) \langle |FT_{nk} I(x, y) - S(x, y)|^2 \rangle \\ &= \lim_{N_x, N_y \rightarrow \infty} \lim_{M \rightarrow \infty} \frac{(N_x N_y \Delta x \Delta y)}{M} \sum_{m=1}^M |FT_{nk} I(x, y) - S(x, y)|^2 \\ &= \lim_{N_x, N_y, M \rightarrow \infty} \frac{\Delta x \Delta y}{M \cdot N_x N_y} \sum_{m=1}^M \left\langle \left| \sum_{i=1}^{N_x} \sum_{j=1}^{N_y} (I(x_i, y_j) - S(x, y)) \exp(-2\pi i(u_n x_i + v_k y_j)) \right|^2 \right\rangle \end{aligned} \quad (6)$$

where  $u$  and  $v$  are the spatial frequencies in the X and Y directions, respectively;  $N_x$  and  $N_y$  are the pixel numbers in the X and Y directions, respectively;  $\Delta x$  and  $\Delta y$  are the spacing in pixels in the X and Y directions, respectively;  $I(x_i, y_j)$  is the intensity of the image at the  $(x_i, y_j)$  pixel location; and  $S(x, y)$  is the mean intensity. Finally, NNPS is obtained using the above-mentioned NPS equation and is calculated as follows:

$$\text{NPS}_{\text{normalized}}(u, v) = \frac{\text{NPS}(u, v)}{(\text{mean signal of average ROI})^2} \quad (7)$$

In addition, we used CNR and COV to evaluate the image performance between the contrast or signal and noise. CNR and COV are calculated as follows [14]:

$$\text{CNR} = \frac{|S_T - S_B|}{\sqrt{\sigma_T^2 + \sigma_B^2}} \quad (8)$$

$$\text{COV} = \frac{\sigma_T}{S_T} \quad (9)$$

where  $S_T$  and  $\sigma_T$  are the mean and standard deviation of the target

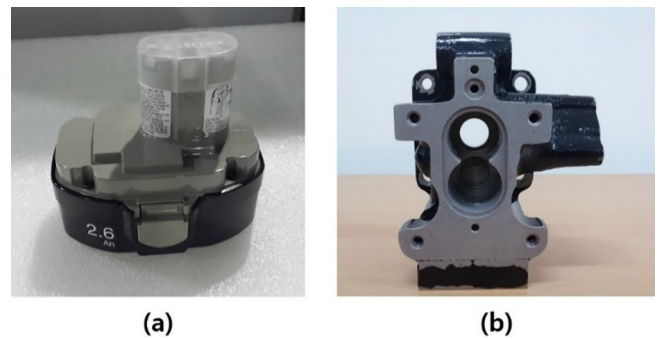


Fig. 3. Photos of the two test phantoms used for evaluating the image performances with our X-ray system: (a) battery and (b) air pump.

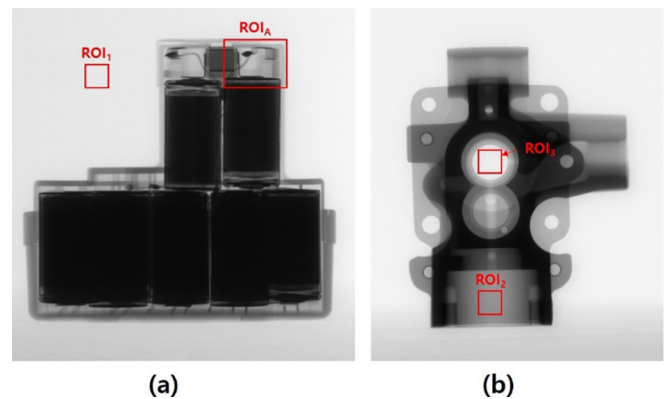


Fig. 4. Examples of test phantom images using (a) battery and (b) air pump with ROIs. NNPS, CNR, and COV were evaluated after setting ROI<sub>1</sub>, ROI<sub>2</sub>, and ROI<sub>3</sub>.

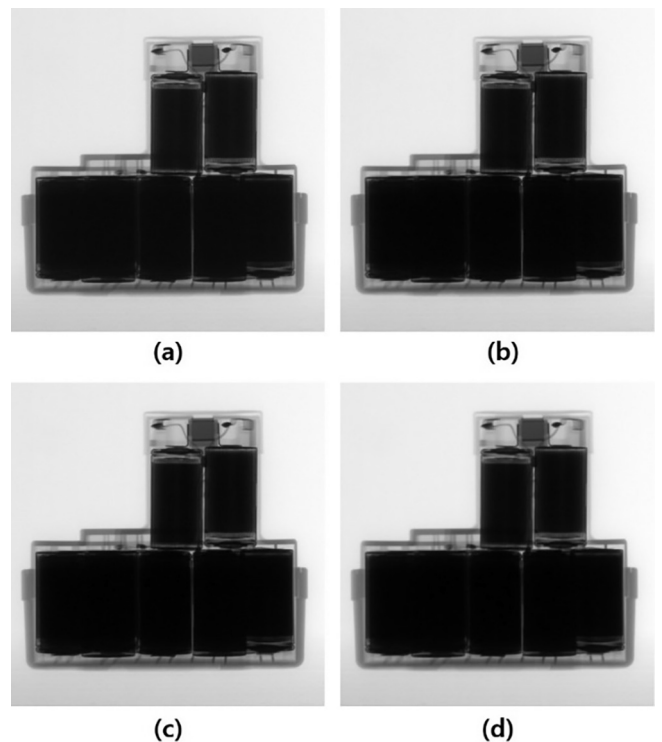


Fig. 5. Images resulting from using the battery test phantom: (a) original with noise, (b) median filter, (c) Wiener filter, and (d) the proposed TV noise reduction algorithm.

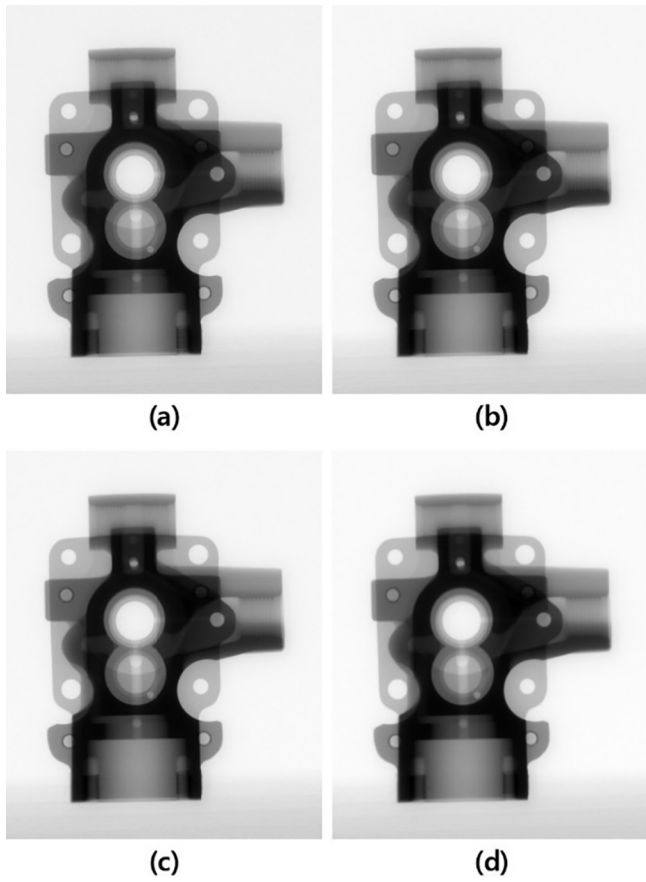


Fig. 6. Images resulting from using the air pump test phantom: (a) original with noise, (b) median filter, (c) Wiener filter, and (d) the proposed TV noise reduction algorithm.

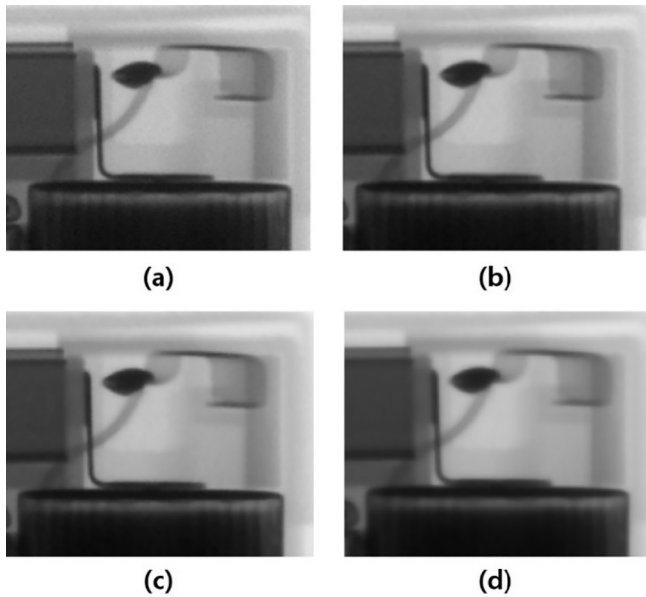


Fig. 7. Magnified test phantom images (using ROI<sub>A</sub> in Fig. 4) with our established high-energy industrial X-ray imaging system using (a) original with noise, (b) median filter, (c) Wiener filter, and (d) the proposed TV noise reduction algorithm.

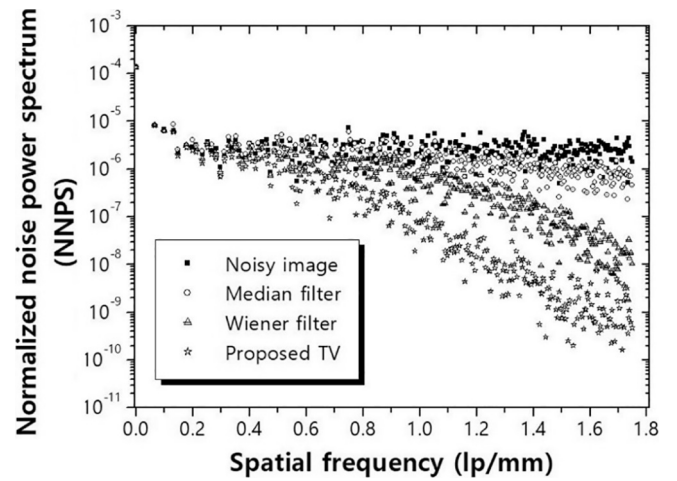


Fig. 8. NNPS results (using ROI<sub>1</sub> in Fig. 4) for the noisy image, median filter, Wiener filter, and our proposed TV noise reduction algorithm.

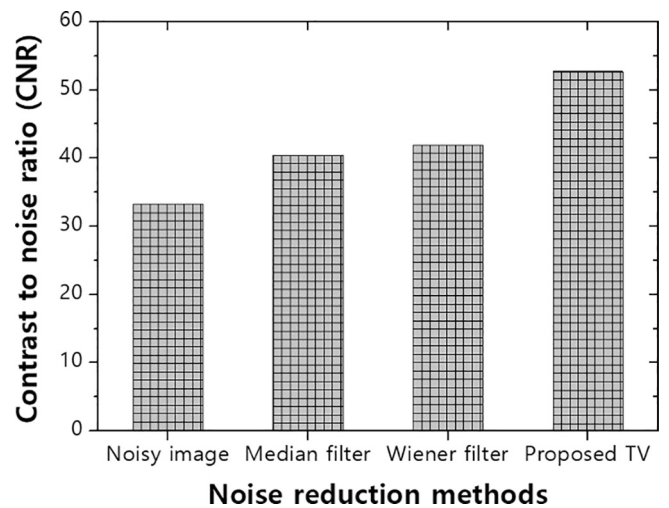


Fig. 9. CNR results (using ROI<sub>2</sub> and ROI<sub>3</sub> in Fig. 4) for noisy image, median filter, Wiener filter, and our proposed TV noise reduction algorithm.

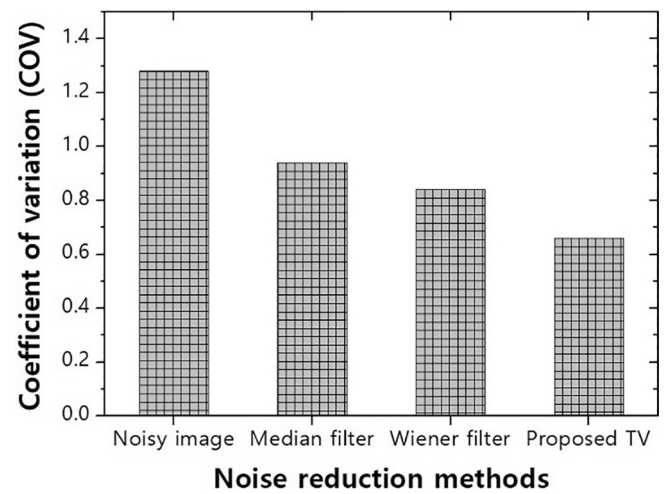


Fig. 10. COV results (using ROI<sub>2</sub> in Fig. 4) for noisy image, median filter, Wiener filter, and our proposed TV noise reduction algorithm.

region of interest (ROI), respectively and  $S_B$  and  $\sigma_B$  are the mean and the standard deviation for the background ROI, respectively. For evaluating image performances, we acquired two test phantom images using our X-ray system: battery and air pump, as shown in Fig. 3.

## Results and discussion

X-ray detection with the NDT method plays an important role in the industry to find faults inside objects. The X-ray imaging systems have gradually achieved higher fault detection efficiency. Among these systems, the high-energy X-ray imaging system using 450 kVp or 3 MeV is widely used. However, noise, which results in degradation of the image performance and fault detection, in the image inevitably occurs in X-ray imaging systems. To improve the image performance, many researchers are actively studying the development of noise reduction algorithms [10–12]. Among these algorithms, the TV-based method based on the regularization technique with the  $L_1$ -norm estimation, has a high efficient noise removal ratio. Therefore, the aim of this study is to establish a high-energy industrial X-ray imaging system using 450 kVp energy and to confirm the application feasibility in our system for the designed efficient TV noise reduction algorithm.

Fig. 4 shows an example of the test phantom images with our established high-energy industrial X-ray imaging system including ROI for the calculation of NNPS (ROI<sub>1</sub>), CNR (ROI<sub>2</sub> and ROI<sub>3</sub>), and COV (ROI<sub>2</sub>). Figs. 5 and 6 show the images resulting from various noise reduction algorithms using the battery and air pump test phantoms, respectively, and Fig. 7 shows the magnified resulting images (ROI<sub>A</sub>) using the various noise reduction algorithms. Based on the magnified images, it is possible to confirm that the noise is reduced from the image using our TV noise reduction algorithm.

Fig. 8 shows the NNPS result using ROI<sub>1</sub> with respect to the noise reduction algorithm. The results of NNPS show that the value of NNPS for the TV noise reduction algorithm is the lowest (approximately  $10^{-10}$  mm<sup>2</sup>) and about  $10^5$  times lower than for the original noisy image. We confirmed that our proposed TV noise reduction algorithm can reduce the noise intensity to a much greater degree and improve the image performance.

The evaluated CNR results for various noise reduction algorithms are shown in Fig. 9. The evaluated CNR obtained from the noisy image, median filter, Wiener filter, and our proposed TV noise reduction algorithm increased in this order. By comparing with the noise reduction methods, the average CNR result using our proposed TV noise reduction algorithm was 1.58, 1.30, and 1.26 times higher than that of the noisy image, median filter, and Wiener filter, respectively. The evaluated COV result for various noise reduction algorithms is shown in Fig. 10. The evaluated COV increased for our proposed TV noise reduction algorithm, Wiener filter, median filter, and noisy image. By comparing with the noise reduction methods, the average COV result using our proposed TV noise reduction algorithm was 1.93, 1.42, and 1.27 times higher than that of the noisy image, median filter, and Wiener filter, respectively. According to the CNR and COV results, our proposed TV noise reduction algorithm can improve the 450 kVp high-energy

industrial X-ray imaging.

Our TV noise reduction algorithm is the most suitable in high-energy industrial X-ray imaging systems. It can efficiently reduce the X-ray image noise compared with conventional filtering methods such as median or Wiener filters due to the regularized term with the  $L_1$ -norm estimation of the constraints of the acquired data. Further, the improved result reflects the correction and iterative steps with the functional space modelling and the integrable functions in our proposed algorithm. Therefore, these results demonstrate that the TV noise reduction algorithm can be used to achieve an appropriate image performance for a 450 kVp high-energy industrial X-ray imaging system. Moreover, the superior noise performance obtained with the proposed noise reduction algorithm is expected to achieve short scan times and low patient doses.

## Conclusion

In this study, we have established a 450 kVp high-energy X-ray imaging system for industrial NDT. To improve the image performance of this system, we designed a TV noise reduction algorithm and investigated the efficiency for image restoration using the calculation of NNPS, CNR, and COV in two test phantoms. The images using our proposed TV noise reduction algorithm were much more clearly restored and visible compared with the conventional filtering methods. In conclusion, our results demonstrate that our proposed TV noise reduction algorithm offers an appropriate image performance of high-energy X-ray imaging system in terms of the various image performance parameters for fault detection in the internal structure of a specimen and the material composition.

## Acknowledgment

This research was supported by the National Research Foundation of Korea (NRF-2016R1D1A1B03930357).

## References

- [1] Ritter F, Boskamp T, Homeyer A, Laue H, Schwier M, Link F, et al. *IEEE Pulse* 2011;2:60.
- [2] Reed AB. *J Vasc Surg* 2011;53:3S.
- [3] Cho HM, Cho HS, Kim KS, Lim HW, Park SY, Lee SR, et al. *NDT&E Int* 2015;75:1.
- [4] Bartscher M, Hilpert U, Goebbels J, Weidemann G. *CIRP Ann* 2007;56:495.
- [5] Kim K, Park S, Kim G, Cho H, Je U, Park C, et al. *Instrum Sci Technol* 2017;45:248.
- [6] Miceli A, Thierry R, Bettuzzi M, Flisch A, Hofmann J, Sennhauser U, et al. *Nucl Instrum Methods Phys Res A* 2007;580:123.
- [7] Chiffre LD, Carmignato S, Kruth JP, Schmitt R, Weckenmann A. *CIRP Ann* 2014;63:655.
- [8] Chatterjee P, Milanfar P. *IEEE Trans Image Process* 2010;19:895.
- [9] Kim SH, Seo K, Kang SH, Bae S, Kwak HJ, Hong JW. *J Magn* 2017;22:570.
- [10] Rudin LI, Osher S, Fatemi E. *Phys D* 1992;60:259.
- [11] Kwak HJ, Lee SJ, Lee Y, Lee DH. *J Instrum* 2018;13. <http://dx.doi.org/10.1088/1748-0221/13/01/T01006>.
- [12] Mukherjee S, Farr JB, Yao W. *Int J Image Process* 2016;10:188.
- [13] Dobbins III JT, Samei E, Ranger NT, Chen Y. *Med Phys* 2006;33:1466.
- [14] Kim D, Park SW, Kim DH, Yoo MS, Lee Y. *Optik* 2018;161:270.